

## Observation of Charge-Exchange Spectra on $C^{6+}+H$ in Low-Energy Collision

KOBUCHI Takashi, SATO Kuninori, GOTO Motoshi, OHYABU Nobuyoshi, KAWAHATA Kazuo,  
SUDO Shigeru, MOTOJIMA Osamu and LHD Experimental Group  
*National Institute for Fusion Science, Toki 509-5292, Japan*

(Received: 11 December 2001 / Accepted: 23 August 2002)

### Abstract

The extreme ultraviolet spectra of C VI have been studied for a Neutral Beam Injection (NBI) plasmas in Large Helical Device (LHD). A strong distortion in the population distribution over the excited levels was observed and we conclude that is caused by charge-exchange recombining (CXR) processes between  $C^{6+}$  ion and recycling neutral hydrogen. Spatially resolved measurements show that the  $C^{6+}$ -H CXR processes take place in the plasma peripheral region in LHD. We have taken a CXR part of C VI 1s-4p line using the result of a calculation code.

### Keywords:

charge exchange recombination (CXR), low-energy collision,  $C^{6+}+H$ , collisional-radiative model (CRM), LHD

### 1. Introduction

Charge-exchange recombination (CXR) cross-sections of highly-ionized ions with neutral hydrogen, which can have the order of  $10^{-15}$  cm<sup>2</sup>, are one of the largest atomic collision processes in plasmas. This CXR process:  $A^{+q} + H^0 \rightarrow A^{+(q-1)*} + H^+$  and the subsequent transitions (termed as charge-exchange spectroscopy (CXS)) have been intensively studied in atomic physicists and plasma spectroscopists [1-3]. Especially as a plasma diagnostics in fusion plasma, CXS using Neutral Beam Injection (NBI) provides capabilities of Doppler ion temperature, plasma rotation, impurity density and transport measurements [4].

Besides the high-energy neutral beam, there exist neutral hydrogen having low energy ( $E < \text{a few tens eV}$ ) in plasmas. These hydrogen atoms can be classified into two kinds [5,6] as follows. (1) Cold particles by gas puffing. Since most of the neutral hydrogen is produced by Frank-Condon dissociation, this energy is about 3 eV. (2) Recycling particles. These are mainly produced

by charge-exchange neutrals reflecting on the wall surface or by plasma bombardment. These recycling particles may have higher energies ( $\sim \text{a few tens eV}$ ) than Frank-Condon neutral and can deeply penetrate into the plasma [5].

In the case of CXR in low-energy collisions, the electron is selectively captured into a single low-excited level of ions. State-selective single-electron capture between hydrogen atom and fully-stripped ion has been so far investigated experimentally and theoretically [7]. It is known that the principal quantum number  $n$  of the ions, to which the electrons are selectively captured in low energy collisions, is determined by the charge  $q$  and is irrespective of the ion species [8]. For  $C^{6+} + H$  collisions, the dominant level of electron capture is  $n = 4$  [7].

In this paper, we discuss CXR on  $C^{6+} + H$  in low-energy collision. We have carried out spatially resolved measurements, and it is confirmed that the reacting

---

Corresponding author's e-mail: kobuchi@nifs.ac.jp

region of CXR processes is in the plasma periphery region. Next, we have calculated C VI intensity distribution from the computer code, and have compared them with the experimental results. Finally, we discuss a mechanism occurring the CXR in the low-energy collision.

## 2. Collisional-Radiative Model Calculation

The emission line intensity distribution of C VI Lyman series has been calculated with the COLRAD code [9]. COLRAD code is a collisional-radiative model code for hydrogen-like ions which solves the coupled rate equations about the time derivatives of the excited level populations. Assuming the quasi-steady-state approximation, the population densities of the excited levels are obtained for a given set of electron temperature and density.

Figure 1 shows the C VI line intensity ratios  $I(Ly\beta)/I(Ly\alpha)$  and  $I(Ly\gamma)/I(Ly\beta)$  calculated using COLRAD code for the plasma parameter range of  $n_e = 10^{12} - 10^{14} \text{ cm}^{-3}$  and  $T_e = 10 - 1000 \text{ eV}$ . Only the ionizing plasma component, which is proportional to the density of ground state of Be-like ion, is shown. These results little depend on  $n_e$ , and in the  $T_e$  range of 100 eV to 1000 eV,  $T_e$  dependence is also small: the intensity ratios show  $I(Ly\beta)/I(Ly\alpha) = 0.09 \pm 0.03$ ,  $I(Ly\gamma)/I(Ly\beta) = 0.26 \pm 0.03$ . The parameters in the emission region of  $C^{5+}$  ions are thought to be in the above ranges, so the intensity ratios of Lyman series are expected to be independent on both of  $T_e$  and  $n_e$  in our experiment.

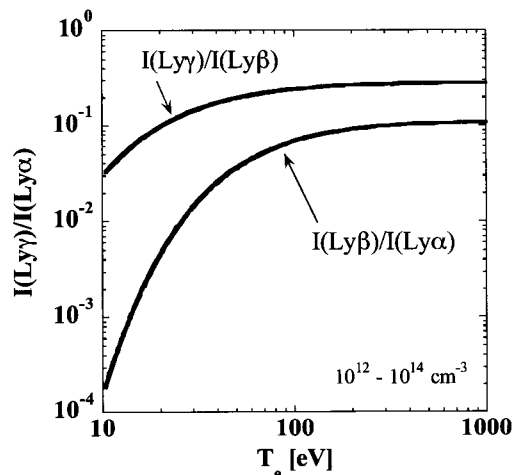


Fig. 1 Emission ratio  $I(Ly\beta)/I(Ly\alpha)$  and  $I(Ly\gamma)/I(Ly\beta)$  calculated using COLRAD code at  $n_e = 10^{12} - 10^{14} \text{ cm}^{-3}$  and  $T_e = 10 - 1000 \text{ eV}$ .

## 3. Experimental Arrangement

LHD is a large heliotron type device ( $l/m = 2/10$ ) using super conducting coils with a nominal major radius  $R$  of 3.9 m, a minor radius  $a$  of 0.6 m and magnetic field strength of  $\sim 3 \text{ T}$ . The electron density  $n_e$  of  $\sim 1.2 \times 10^{14} \text{ cm}^{-3}$  and electron temperature  $T_e$  of  $\sim 4.5 \text{ keV}$  have been achieved with NBI of 3 MW and pellets injection.

In LHD, an impurity is monitored using a 2m grazing incidence spectrometer (Schwob-Fraenkel type spectrometer), which is equipped with two multichannel detectors. The wavelength coverage is 0.5–34 nm with a resolution of 0.02 nm using a 600 grooves/mm grating. This XUV spectrometer is installed at the end of manifold for the vacuum pumping system of LHD. The neutral beams do not cross the field of view of the spectrometer.

To move the field of view, spectrometer is rotated around a pivot located 1 meter ahead from the entrance slit. Figure 2 shows the line-of-sight for spatially resolved measurements using the XUV spectrometer. The last closed flux surface (LCFS) and the ergodic layer in vacuum magnetic field on magnetic axis position  $R_{ax} = 3.75 \text{ m}$  are shown in Fig. 2. The fields of view for the measurements at the plasma center and edge region are also shown. In the case of center view, the line-of-sight crosses the X-points and the thick part of the ergodic layer. The line-of-sight of 500 mm height monitors mainly the ergodic layer.

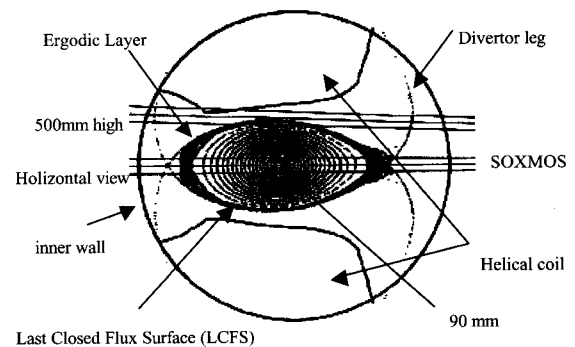


Fig. 2 The line-of-sight of spectrometer.

## 4. Results and Discussion

### 4.1 A "distortion" in the regular decrement of the Lyman series

Typical spectra of C VI Lyman series observed with the line-of-sight at the plasma center with exposure time for 0.4 sec are shown in Fig. 3. Figure 3(b) shows a "distortion" in the regular decrement for  $Ly\gamma$  line. Though the relative intensity of  $Ly\beta$  to  $Ly\alpha$  is consistent with the theoretical prediction, the intensity ratio of  $Ly\gamma$  to  $Ly\beta$  reaches to 0.9, it deviates far from the expected value of 0.3. The result suggests an additional electron populating processes to  $n = 4$  level of  $C^{5+}$  ion.

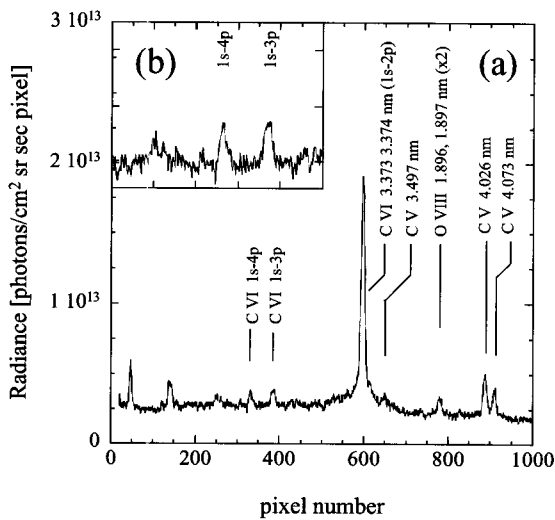


Fig. 3 Typical spectra of C VI Lyman series.

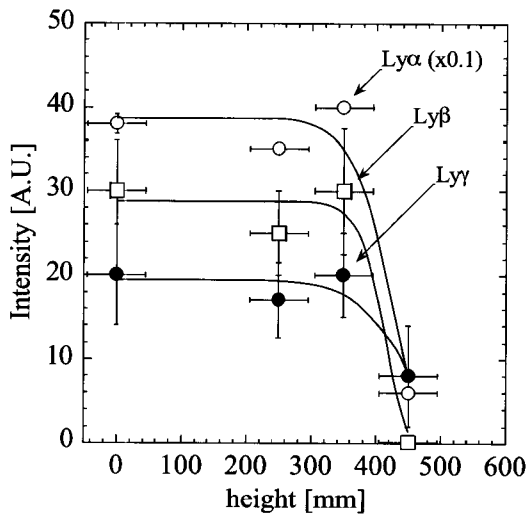


Fig. 4 Spatially resolved distribution of Lyman series spectra.

### 4.2 Spatially resolved intensity measurement

In order to investigate the reacting region for  $C^{6+}-H$  charge-exchange collision, spatially resolved intensity measurements were tried shot by shot for C VI Lyman series spectra, and an intensity distribution of C VI series is shown in Fig. 4. A chordal radius, the perpendicular distance from the magnetic axis to the chordal view of the spectrometer at magnetic axis, was scanned from 0 to 500 mm. The measurements were made in a series of nominally identical NBI heating plasma with the total stored plasma energy  $W_p \sim 0.4$  MJ, the line averaged electron density  $n_e \sim 2-3 \times 10^{13} \text{ cm}^{-3}$ , the total radiation power  $P_{\text{rad}} \sim 0.5$  MW, magnetic field  $B_t = 2.75$  T and magnetic axis  $R_{\text{ax}} = 3.6$  m. Solid lines in the figure are fitted results of the measurement. The fitted lines of  $I(Ly\beta)$  and  $I(Ly\gamma)$  are within the errors of the measurement, but this is not the case for  $I(Ly\alpha)$ . The relatively smaller values at 250mm might be caused by the slightly different plasma conditions, so we don't think that they indicate a change in the emission profile.

The spatial profiles of  $Ly\alpha$  and  $Ly\beta$  intensities present hollow shapes, and both intensities steeply decrease in the plasma peripheral region, at around 350 mm height in chord radius. On the other hand, the intensity distribution of  $Ly\gamma$  is different from the other lines. An intensity inversion between  $Ly\beta$  and  $Ly\gamma$  is seen at around the chordal view of 450 mm height.

In order to make clear the region where the  $C^{6+}-H$  CXR processes predominantly take place, the Abel inversion is carried out using the fitting lines in Fig. 4. Intensity contour is defined using the vacuum magnetic

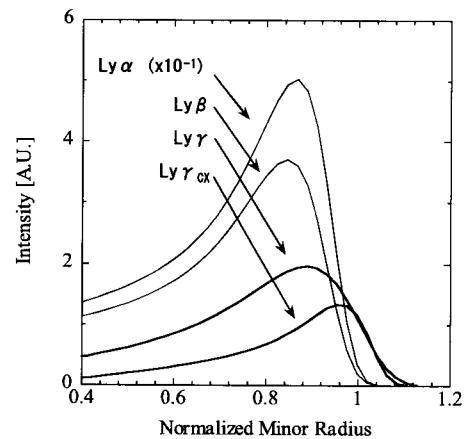


Fig. 5 Radial profiles of observed emission intensity of  $Ly\alpha$ ,  $Ly\beta$  and  $Ly\gamma$ . These are calculated using Abel inversion method.  $Ly\gamma_{\text{CX}}$  has been estimated from the relation between  $Ly\beta$  and  $Ly\gamma$  on CRM.

surface in magnetic axis position  $R_{ax} = 3.6$  m. In the outside region of LCFS ( $\rho > 1.0$ ), it is simply assumed that a closed magnetic surface still exists. Figure 5 shows the Abel-inverted radial emission profiles of Lyman series. The radial profiles of Ly $\alpha$  and Ly $\beta$  have the same shape and peak position at normalized minor radius  $\rho = 0.9$ . The peak position of Ly $\gamma$  is located at outside those of Ly $\alpha$  and Ly $\beta$ .

We have tried to pick up the CXR component (Ly $\gamma_{CX}$ ) from the measured Ly $\gamma$  intensity. We define  $I(Ly\gamma_{CX})$  as follows:

$$I(Ly\gamma_{CX}) = I(Ly\gamma) - 0.26 \times I(Ly\beta), \quad (1)$$

where the value of 0.26 is the normal ratio (see. Fig. 1). This assumption is reasonable for our experiment because the electron temperature is a few hundreds eV at the ergodic layer and the peak of the radial profile of C<sup>5+</sup> exists at the inside the ergodic layer. The right-hand side of Eq. (1) represents the difference between the measured Ly $\gamma$  and the intensity calculated with CRM. The emission profile of Ly $\gamma_{CX}$  is also shown in Fig. 5. This differs from the emission profile of Ly $\alpha$  and Ly $\beta$ , and peak position is located at outside those of Ly $\alpha$  and Ly $\beta$ . The emission profile of Ly $\gamma_{CX}$  suggests the reacting region of the CXR processes.

## 5. Conclusion

We have shown the characteristics of the CXR of carbon ions in low-energy collisions and have found CXR spectrum which originates from the low-energy collision on C<sup>6+</sup> + H system. Using the spatially resolved measurements and Abel inversion technique, the reacting region in the low-energy collision on C<sup>6+</sup> + H system is found at peripheral region. Comparing the results of COLRAD code with the relative intensity of Ly $\beta$ , we estimate CXR component in the measured Ly $\gamma$  line intensity.

In order to investigate a behavior of recycling particles and the influence to plasma confinement, we must take a plasma parameter condition in which the CXR process occurs in the low-energy collision on C<sup>6+</sup>

+ H system. We try to reproduce the measured distribution in decrement of C VI Lyman series emission from COLRAD code with CXR process. Assuming that the condition from COLRAD code with CXR process is taken, we may understand a mechanism in which the CXR occurs in low-energy collisions in detail.

In order to extend the discussion, we have to investigate a wide range of plasma parameter and other elements. We expect to observe the same characters about other elements, oxygen etc. If other elements are also observed with the same characters, the measurement of such as a distinctive feature may be used for the observation of a behavior and density of recycling particles by comparing the results of a model calculation with the CXR process at more central region.

## Acknowledgements

We are grateful to technical staffs for their help in operating the LHD, NBI, ECRH and diagnostics. And we also wish to thank for the other members of LHD group.

## References

- [1] R.C. Isler, *Phys. Rev. Lett.* **38**, 1359 (1977).
- [2] R.K. Janev, D.E. Belie and B.H. Bransden, *Phys. Rev. A* **28**, 1293 (1983).
- [3] R.C. Isler, *Plasma Phys. Control. Fusion* **36**, 171 (1994).
- [4] K. Ida and S. Hidekuma, *Rev. Sci. Instrum* **60**, 876 (1989).
- [5] Y. Nakashima *et al.*, *J. Phys. Soc. Jpn.* **52**, 4166 (1983).
- [6] H. Takahashi *et al.*, *J. Phys. Soc. Jpn.* **44**, 1363 (1978).
- [7] N. Toshima and H. Tawara, *NIFS-DATA-26*.
- [8] M. Kimura *et al.*, *J. Phys. Soc. Jpn.* **53**, 2224 (1984).
- [9] N.N. Ljepojevic, R.J. Hutcheon and J. Payne, *Computer Physics Communications* **44**, 157 (1987).